1983

A Pore Water/Solid Phase Diagenetic Model for Manganese in Marine Sediments

David J. Burdige
Old Dominion University, dburdige@odu.edu

Joris M. Gieskes

Original Publication Citation

Burdige, D.J., & Gieskes, J.M. (1983). A pore water/solid phase diagenetic model for manganese in marine sediments. *American Journal of Science, 283*(1), 29-47. doi: 10.2475/ajs.283.1.29

[AMERICAN JOURNAL OF SCIENCE, VOL. 283, JANUARY, 1983, P. 29-47]

A PORE WATER/SOLID PHASE DIAGENETIC MODEL FOR MANGANESE IN MARINE SEDIMENTS

DAVID J. BURDIGE and JORIS M. GIESKES

Scripps Institution of Oceanography, La Jolla, California 92093

ABSTRACT. A steady state diagenetic model is developed which accounts for changes in both the pore water and solid phase manganese profiles in marine sediments as a result of advection, diffusion, and redox reactions. The model is applied to observations on two cores in the eastern equatorial Atlantic in which pore water and solid phase manganese data are available. In-situ *reaction rates for manganese oxidation and reduction are estimated. The oxidation rates calculated here are in good agreement with rates measured in laboratory studies. In addition, the calculated manganese oxidation and reduction rates are compared with other estimated rates for these processes in natural environments.*

INTRODUCTION

Oxidation-reduction processes involving manganese have long been the subject of intensive research in marine chemistry. In addition to field measurements in sediments (Lynn and Bonatti, 1965; Li, Bischoff, and Mathieu, 1969; Bischoff and Sayles, 1972; Robbins and Callender, 1975; Holdren, Bricker, and Matisoff, 1975; Froelich and others, 1979; Aller, 1980; Emerson and others, 1980; and others) recent studies (primarily in the water column) have focused on the dynamics of these redox reactions and the possible role microorganisms (primarily bacteria) may play in catalyzing these reactions (Wollast, Billen, and Duinker, 1979; Nealson, 1983; Emerson and others, 1982).

For fresh water and marine sediments Robbins and Callender (1975) and Holdren, Bricker, and Matisoff (1975) have presented mathematical models for manganese diagenesis, although as we will discuss below, neither of these is appropriate for sediments in which oxidation and reduction occur over finite depth intervals. In addition, these models do not directly address the effect of these redox reactions on the solid phase profiles.

In this paper we present a mathematical model for steady state manganese diagenesis which accounts for changes in both pore waters and solids due to advection, diffusion, and redox reactions. The reaction rates obtained from this modeling procedure, when combined with appropriate laboratory data on the mechanisms of these reactions and/or other measured quantities, should lead to a better understanding of the dynamics of manganese redox reactions and help delineate the importance of bacterial catalysis (as opposed to inorganic chemical reactions) in these transformations.

PREVIOUS MODELS

Several mathematical models for manganese diagenesis in sediments have been presented previously (Michard, 1971; Robbins and Callender, 1975; Holdren, Bricker, and Matisoff, 1975), though for a number of

reasons they are not appropriate for most marine sediments. The models of Robbins and Callender (1975) and Holdren, Bricker, and Matisoff (1975) have been developed for essentially totally anoxic sediments underlying aerobic waters, where manganese oxidation is restricted to the sediment-water interface. While this characterization is almost certainly valid for the environments they have studied (Lake Michigan and Chesapeake Bay), it is not generally applicable to marine sediments, which may be aerobic to a wide range of depths below the sediment-water interface and in which manganese oxidation may be important over all or part of this zone.

In addition, neither of these models directly addresses the relationship between changes in pore waters and solids due to chemical reactions between them. We believe that such considerations are essential because the chemical reactions involving manganese which are thought to be important in the uppermost part of marine sediments (generally less than one meter) involve transfer of manganese between pore waters and solids. Most simply, these reactions can be expressed by:

$$Mn^{2+}\ (\text{soluble}) \underset{\text{reduction}}{\overset{\text{oxidation}}{\rightleftharpoons}} MnO_x\ (\text{solid hydrous oxide}) \qquad (1)$$

where x is generally less than 2 (Morgan, 1967) and may be as low as 1.33 (Klinkhammer and Bender, 1980).

Michard (1971) on the other hand, considers a sedimentary environment with finite oxidizing and reducing zones and derives a set of equations to explain changes in both the solids and pore waters. However, he assumes that in the reducing zone, manganese reduction occurs instantaneously and that adsorption and equilibrium with a carbonate phase control dissolved manganese. As we will discuss below, this is probably not a valid representation.

THE PRESENT MODEL

Qualitative description of the sediments

For the purposes of our model, we have divided the sedimentary column into four distinct zones (illustrated in fig. 1) which are unique in both their physicochemical conditions and manganese chemistry. As this description is virtually identical with that of Klinkhammer (1980), we have chosen to use his terminology for the upper three regions. Briefly, they are:

1. *Oxidized zone ($0<z<L1$).*—In this zone, dissolved Mn^{2+} is essentially zero. Any dissolved manganese that diffuses across the redox boundary (at $z = L2$) is entirely consumed (by oxidation) before it reaches this zone. If the input of solid manganese to the sediments is constant with time, then in this region solid manganese should be constant with depth.

2. *Manganese oxidation zone ($L1<z<L2$).*—Here the dissolved manganese profile increases with depth and is concave upward (that is, shows negative curvature) because of diffusion of Mn^{2+} across the redox boundary and consumption via oxidation. Because the product of oxidation is

a solid hydrous manganese oxide which we have termed MnO_x, there is an increase with depth in the solid manganese profile.

3. *Manganese reduction zone (L2<z<L3).*—As solid manganese is buried below the redox boundary, manganese reduction becomes the favored reaction. There are two possible explanations for this. As oxygen and NO_3^- are consumed in bacterial metabolic reactions, it is thought that MnO_2 may become the next preferred electron acceptor, in terms of maximizing the free energy gained from oxidizing organic matter (Claypool and Kaplan, 1974; Froelich and others, 1979; Emerson and others, 1980). While this explanation is consistent with pore water data and thermodynamic calculations, the data are also consistent with the explanation that in this zone Eh-pH conditions change (perhaps induced by bacterial activity) so that now Mn^{2+} is favored over solid manganese oxide-hydroxides. While the resolution of this question certainly bears further investigation, the qualitative result (in terms of manganese profiles) of either process is the same. Pore water manganese profiles are concave downward (showing negative curvature) due to production via dissolution and increase with depth, while solid manganese decreases with depth.

4. *Equilibrium zone (z>L3).*—At z = L3, dissolved manganese reaches a maximum and may actually decrease with depth (Li, Bischoff, and Mathieu, 1969; Robbins and Callender, 1975; Holdren, Bricker, and Matisoff, 1975; Aller, 1980). Equilibrium calculations have shown that pore waters of the region should be supersaturated with respect to rhodochrosite ($MnCO_3$) or a mixed phase (Ca, Mg, Mn) carbonate (Li, Bischoff, and Mathieu, 1969; Holdren, Bricker, and Matisoff, 1975; Aller, 1980; Klinkhammer, 1980). Although these solid phases have generally not been

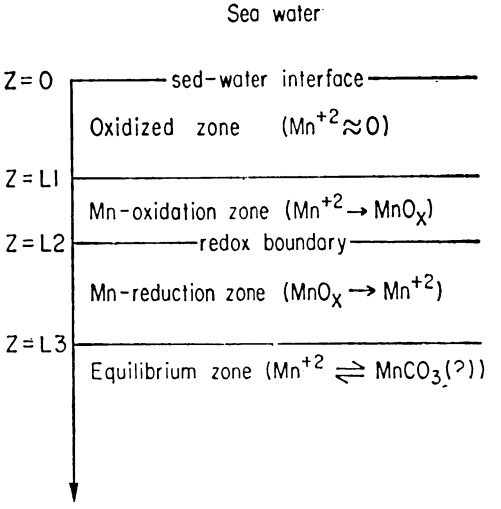

Fig. 1. Schematic illustration of the zonation of marine sediments with regard to manganese geochemistry.

detected, equilibrium with such phases is thought to control the concentration of dissolved manganese in this region.

In our model, we will only concern ourselves with the oxidation and reduction zones, although when actually applying the equations to real data we will have to determine the boundary between oxidized and oxidation zones (that is, what is the value for L1). We will not concern ourselves with modeling the equilibrium zone, as this problem has been previously considered (Robbins and Callender, 1975; Holdren, Bricker, and Matisoff, 1975).

In addition to these zones, we have also defined a "redox boundary" at z = L2. In its simplest terms, this should be the depth in the sediments below which Mn^{2+} is favored over solid manganese oxide phases. In any system, this boundary can easily be determined by comparison of the pore water and solid manganese data with theoretical profiles (see fig. 2), since each shows distinctive characteristics in the region. In addition, these profiles can also be compared with pore water nitrate profiles to determine this boundary, since nitrate is usually significantly depleted (due to bacterial denitrification) at the depth at which manganese reduction becomes important (Froelich and others, 1979; Emerson and others, 1980).

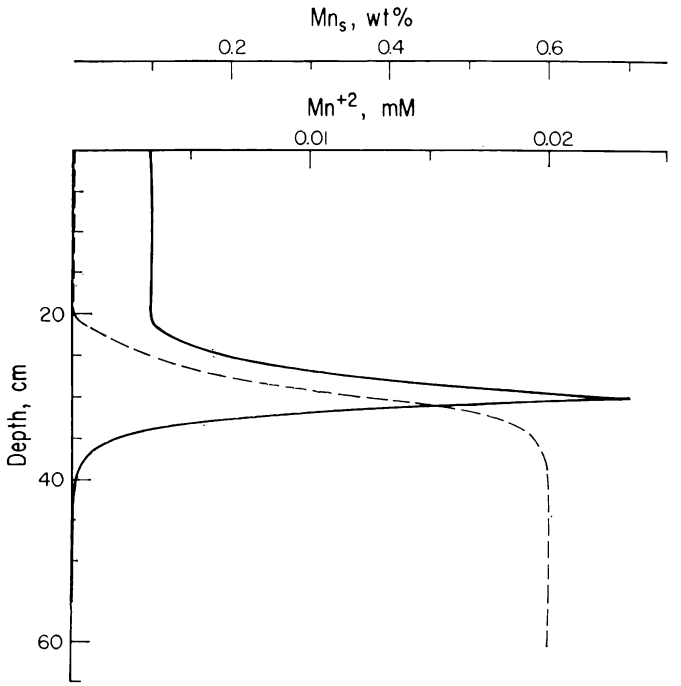

Fig. 2. Theoretical pore water (dotted line) and solid phase (solid line) manganese profiles predicted by eqs (17) to (26) using the following parameters: D_b = 71.6 cm^2/yr, w = 3 cm/10^3 yrs, ϕ = 0.8, ρ = 2.6 gr/cm^3/sed, L1 = 20 cm, L2 = 30 cm, $C_s°$ = 0.1 wt%, k_{ox} = 5 yr^{-1}, and $k_{red} = 1.50 \times 10^{-3}$ yr^{-1}.

Derivation of diagenetic equations

This qualitative description can be translated into a quantitative mathematical model, using the following steady state diagenetic equations (Berner, 1980):

$$D_b \frac{\partial^2 C_p}{\partial z^2} - w \frac{\partial C_p}{\partial z} + R(z) = 0 \quad (2)$$

$$-w \frac{\partial C_s}{\partial z} - \frac{\phi}{1-\phi} R(z) = 0 \quad (3)$$

where D_b is the bulk sediment diffusion coefficient (identical with Berner's D_s), C_p is the concentration of manganese in the pore waters, C_s is the

TABLE 1

Parameters used for fitting data from 14 GC1 and 16 GC1 to eqs (17) to (20)

Parameter	Value (uncertainty or range)	How obtained
D_b (bulk sediment diffusion coefficient)	71.6 cm²/yr (57.3-85.9)	See below*
w (sedimentation rate)	3.8 cm/10^3 yr (3.4-4.2)	^{14}C dating in cores 10 GC1, 5 GC1, and 14 GC1**
ϕ (porosity)	0.77 (± 0.03)	Porosity measurements averaged over the depth of interest**
ρ (density of dried sediment)	2.65 gr_{sed}/cm^3_{sed} (± 0.11)	Calculated with the average measured bulk dry density ($gr_{sed}/cm^3_{bulk\ sed}$) and average porosity**
L1 (upper boundary of oxidizing zone)		Comparison of pore water and solid phase Mn profiles (see text)**
14 GC1	24 cm (± 2)	
16 GC1	27 cm (± 2)	
L2 (redox boundary)		Comparison of pore water Mn^{+2} and NO_3^- and solid phase Mn profiles (see text)**
14 GC1	32 cm (± 2)	
16 GC1	35 cm (± 2)	
$C_s°$ (solid phase Mn at z = 0)***	0.035 wt% (± 0.005)	Solid Mn profile**

* D_b was calculated using $D_b = D/\phi F$ (eq (4)). The value for D was obtained by interpolating the data of Li and Gregory (1974) for the self-diffusion coefficient of Mn^{+2} as a function of temperature. Assuming the temperature of the sediments is 4°C and that D versus T is linear between 0°C and 25°C we obtain $D = 3.5 \times 10^{-6}$ cm²/sec = 110.4 cm²/yr. Based on measured formation factors (Berner, 1980; Burdige and Gieskes, unpub data) we have assumed F = 2. Using $\phi = 0.77$, this implies that D_b is 71.6 cm²/yr, which is similar to manganese bulk sediment diffusion coefficients used by other authors (Bender, 1971; Holdren, Bricker, and Matisoff, 1975; Robbins and Callender, 1975; Klinkhammer, 1980). Given the uncertainties in D, ϕ, and F we believe that a 20 percent uncertainty in D_b is not unreasonable; hence the listed range in D_b.

** The complete pore water and solid phase data as well as bulk sediment data are tabulated in Froelich (ms).

*** Assuming C_p has units of millimoles/$cm^3_{pore\ water}$, dimensional analysis of eqs (7) to (10) shows that C_s has units of millimoles/cm^3_{sed}. Solid concentrations in wt% (g Mn/100 g dried sed.) can be converted to these units using:

$$C_s(\text{millimoles/cm}^3_{sed}) = C_s(\text{wt\%}) \times 10\rho/MW$$

where MW is the atomic weight of manganese (= 55).

concentration of manganese in the solid phase (see note ***) in table 1 regarding the units of C_p and C_s), w is the sedimentation rate, ϕ is the porosity and R(z) is a rate expression for either oxidation or reduction. As shown in figure 1, z is the depth coordinate (relative to the sediment-water interface); the term $\phi/1-\phi$ (which has units $cm^3_{pore\ water}/cm^3_{dry\ sed.}$) is used to convert manganese concentrations between the solid and liquid phases.

Implicit in these equations are the following assumptions:

1. Steady-state diagenesis is present.
2. Vertical gradients are far more important than horizontal ones, and the latter can be ignored.
3. Diffusion in pore waters occurs by molecular processes (that is, follows Fick's Laws).
4. Porosity and diffusion coefficients are constant with depth.
5. Advection is constant and equal to the sedimentation rate.
6. Solid phase diffusion can be neglected.
7. The supply of solid manganese to the surface of the sediments is constant over time.
8. Adsorption of Mn^{2+} can be neglected — as discussed by Robbins and Callender (1975) adsorption is probably insignificant compared to redox reactions (Hem, 1964).
9. Bioturbation by macrofauna can be neglected, since in most marine sediments this process will be concentrated sufficiently close to the sediment-water interface to be above the oxidation (or reducing) zone.

Assumptions (1) to (6) are discussed in greater detail by Berner (1980). As he points out, these are probably valid for modelling sedimentary systems less than a few meters thick.

D_b differs from the free ion diffusion coefficient in seawater (D) because of tortuosity effects due to the presence of sediment particles. D_b can be related to D by the following equation (McDuff and Ellis, 1979):

$$D_b = D/\phi F \tag{4}$$

where F is the "formation factor." This factor is based on the physical analog between electrical conductivity and diffusion and is measured as the ratio of the bulk sediment resistivity to the pore water resistivity alone (McDuff and Ellis, 1979; McDuff and Gieskes, 1976).

In eqs (2) and (3), R(z) is the rate expression for either oxidation or reduction. In the presence of abundant surface area (such as a sediment), manganese precipitation/oxidation has been found to be a pseudo-first order process (Hem, 1963, 1964, 1981; Michard, 1969, 1971) and so

$$R_{ox}(z) = k_{ox}C_p \tag{5}$$

Regardless of whether oxidation is biologically catalyzed or strictly an inorganic reaction, eq (5) should be an appropriate rate expression for oxidation under these conditions. The product of this reaction is presumed to be a hydrous oxide (which we have called MnO_x), although the

existing data on sedimentary manganese mineralogy cannot resolve the exact phase(s) that form under natural conditions.

As we discussed above, manganese reduction in marine sediments may either be due to an inorganic chemical reaction or may be a biological process, coupled to bacterial metabolism and organic matter oxidation. It is also possible that overall reduction is due to some combination of the two processes. In any event, in this paper we will assume that regardless of the exact mechanism the rate of reduction will be proportional to the amount of solid manganese available (which is presumed to be all hydrous oxide). Thus $R_{red}(z)$ can be expressed as:

$$R_{red}(z) = k_{red}C_s \tag{6}$$

which is identical with the rate expression for reduction used by Holdren, Bricker, and Matisoff (1975). If dissolution is an inorganic reaction, then it is common to assume that the rate is proportional to the surface area of the dissolving solid (Wadsworth, 1975). If we also assume that these hydrous oxides are essentially present as two-dimensional coatings on clay particles (Holdren, Bricker, and Matisoff, 1975) then the amount of solid manganese is roughly proportional to the surface area of solid dissolving, and we obtain eq (6).

As Aller (1980) points out, if dissolution of manganese oxides is coupled to bacterial metabolism, then the rate of reaction may be limited by either the availability of manganese oxides or the quantity of organic matter. Given the lack of both laboratory or field data regarding this problem we have chosen to assume that eq (6) is also valid for microbially mediated manganese reduction.

Combining these rate expressions with (2) and (3), we obtain the following sets of equations:

A. For the oxidizing zone ($L1 \leqslant z \leqslant L2$)

$$D_b \frac{\partial^2 C_p^{ox}}{\partial z^2} - w \frac{\partial C_p^{ox}}{\partial z} - k_{ox} C_p^{ox} = 0 \tag{7}$$

$$-w \frac{\partial C_s^{ox}}{\partial z} + \frac{\phi}{1-\phi} k_{ox} C_p^{ox} = 0 \tag{8}$$

B. For the reducing zone ($L2 \leqslant z \leqslant L3$)

$$D_b \frac{\partial^2 C_p^{red}}{\partial z^2} - w \frac{\partial C_p^{red}}{\partial z} + \frac{1-\phi}{\phi} k_{red} C_s^{red} = 0 \tag{9}$$

$$-w \frac{\partial C_s^{red}}{\partial z} - k_{red} C_s^{red} = 0 \tag{10}$$

Solutions to the diagenetic equations

Eqs (7) to (10) can be solved analytically using the following boundary conditions:

1. $$C_p^{ox}(L1) = 0 \tag{11}$$

2. $$C_s^{ox}(L1) = C_s^{o} \tag{12}$$

3. Continuity of concentrations at the redox boundary. This implies that

$$C_p^{ox}(L2) = C_p^{red}(L2) \tag{13}$$

$$C_s^{ox}(L2) = C_s^{ox}(L2) \tag{14}$$

4. Continuity of fluxes across the redox boundary. For the solids, this is equivalent to eq (14), since the only fluxes we are considering are advective in nature (= $(1-\phi)\,wC_s$) and we are assuming ϕ and w are constant over the entire depth of sediments under consideration. In the pore waters, this condition means that

$$\phi w C_p^{ox}(L2) - \phi D_b \left(\frac{\partial C_p^{ox}}{\partial}\right)_{L2} = \phi w C_p^{red}(L2) - \phi D_b \left(\frac{\partial C_p^{red}}{\partial z}\right)_{L2} \tag{15}$$

By eq (13) and the fact that ϕ and w are constant, the advective terms cancel. Since we are also assuming that D_b is constant with depth, this boundary condition simplifies to

$$\left(\frac{\partial C_p^{ox}}{\partial z}\right)_{L2} = \left(\frac{\partial C_p^{red}}{\partial z}\right)_{L2} \tag{16}$$

5. As $z \to \infty$, C_p remains finite.

These boundary conditions are similar to those used by Peng, Takahashi, and Broecker (1974) in modeling radon transfer in surface waters, where they used an analogous two layer model. With these boundary conditions, the solutions to (7) to (10) are

$$C_p^{ox} = A \sinh(\alpha(z-L1)) \tag{17}$$

$$C_p^{red} = G - \frac{1-\phi}{\phi} \frac{Ew^2}{k_{red} D_b} e^{-\beta(z-L2)} \tag{18}$$

$$C_s^{ox} = C_s^{o} \cosh(\alpha(z-L1)) \tag{19}$$

$$C_s^{red} = Ee^{-\beta(z-L2)} \tag{20}$$

where

$$\alpha = \sqrt{k_{ox}/D_b} \tag{21}$$

(assuming $4D_b k_{ox} >> w^2$, that is, advection in pore waters is negligible compared to diffusion) and

$$\beta = k_{red}/w \tag{22}$$

$$L_{ox} = L_2 - L_1 \tag{23}$$

$$A = \frac{C_s^{o}(1-\phi)w}{\phi \alpha D_b} \tag{24}$$

$$E = C_s^{o} \cosh \alpha L_{ox} \tag{25}$$

$$G = A(\sinh \alpha L_{ox} + \alpha/\beta \cosh \alpha L_{ox}) \tag{26}$$

(Note: In eqs (18) and (26) we have also assumed $D_b k_{red} >> w^2$.) The derivation of these equations is discussed in greater detail in the appendix.

In these equations, there are still two unknown parameters (k_{ox} and k_{red}) which can be used to least square fit the equations to actual data. (As discussed in table 1, D_b, w, ϕ, C_s^0, L1, and L2 are all determined from the actual data). A more complete description of the fitting procedure will be given in the section *Application to Real Data.*

APPLICATION OF THE MODEL

Using typical parameters for marine sediments, model profiles calculated with these equations are shown in figure 2. These profiles are very similar to the schematic representation presented by Froelich and others (1979) for a hypothetical steady state system for manganese in marine sediments.

These profiles are also consistent with the manganese post-depositional migration mechanism originally discussed by Lynn and Bonatti (1965). As sediments are buried below the redox boundary, solid manganese oxides are reduced to Mn^{+2}, which diffuses upward (along the concentration gradient) to be eventually oxidized and reprecipitated. With further sedimentation, these redeposited solids are again brought back into the reducing zone to be dissolved once more. The net result of this continual recycling, as discussed by Lynn and Bonatti (1965) and Bender (1971) and shown in figure 2, is that solid manganese is trapped in a relatively narrow zone at the redox boundary.

Application to real data

We have attempted to test the validity of our model by applying it to the data of Froelich and others (1979) on pelagic sediments of the eastern equatorial Atlantic where they have measured detailed pore water *and* solid phase manganese profiles as well as dissolved nutrients (most importantly for our model, nitrate). Attempts to test the model with other data sets have in general been unsuccessful, due to the absence of solid phase Mn data accompanying the pore water results. In the case of the data from Li, Bischoff, and Mathieu (1969) for Arctic basin sediments, where solid phase data are presented, there appear to be at least two additional peaks in the solid profile below the redox boundary which (as discussed below) make the core inappropriate for examination here.

As described in Froelich and others (1979) and summarized in table 2, these sediments showed two distinct zones with a $\approx$ 10 cm zone of transi-

TABLE 2

Description of the sediments from eastern equatorial Atlantic*

	Above 35 cm	Below 35 cm
Color	Tan	Dark olive-green
Lithology	Highly calcareous (70-90% $CaCO_3$) post-glacial sediments	Silty, less calcareous (<60% $CaCO_3$) terrigenous glacial sediments
Organic carbon content	0.2-0.5%	0.5 to >1%

* Based on information from Froelich and others (1979) on gravity cores 10 through 23 GCI. The approximate location of these cores is 0°31′N (±30′), 12°W (±4°).

tion in between. We will assume that in spite of the variation in lithology, manganese diagenesis is in steady state over the entire length of interest (approximately the first 60 cm). In addition, we will assume that within their uncertainties (see table 1) the diffusion coefficient, sedimentation rate, porosity, and bulk dry density of the sediments are also constant over this depth. For a more detailed description of sample collection, analysis, and a general discussion of the pore water results, the reader should consult Froelich and others (1979), Froelich (ms), or Berner (1980, p. 194-198).

In three of these cores (5 GC1, 10 GC1, 23 GC1) there is a second peak in solid manganese occurring in the reducing zone, which Froelich and others (1979) attribute to a possible change in the past in bottom water O_2 or organic matter burial rate. As Froelich and others (1979) state (p. 1086), "The lower solid Mn peak would then be a relict feature which is slowly being reduced and redeposited at the depth of the upper solid Mn peak" (that is, at the redox boundary). As a result, it would seem that these are non-steady state profiles and therefore beyond the scope of this model.

With the two remaining cores (14 GC1 and 16 GC1) that have finite oxidizing zones (that is, L1 $\neq$ L2 $\neq$ 0) we have been able to obtain very good correlations between our equations and the data. The parameters describing the system used in these calculations are listed in table 1. The data for 14 GC1 have been fit to eqs (17) to (20) by adjusting k_{ox} and k_{red} until the variance of the pore water data with these equations is minimized. The rate constants that result from the best fit of the data as well as the resulting constants of integration (A,E,G) are listed in table 3. These results are also plotted in figures 3 and 4.

In an attempt to estimate the uncertainty in k_{ox} and k_{red} we have systematically varied D_b, w, ϕ, ρ, C_s^o, L1, and L2 so that in any one calculation one of the extreme values for a parameter (listed in table 1) is used while the others retain their "normal" values. The averages and un-

TABLE 3

Rate constants and constants of integration for the best fit solutions to the diagenetic equations (eqs 17 to 20)

Constant	14 GC1	16 GC1*
"best fit"		
k_{ox}	12.0 yr^{-1}	10.7 yr^{-1}
k_{red}	2.10×10^{-3} yr^{-1}	1.50×10^{-3} yr^{-1}
A**	6.53×10^{-7}	6.92×10^{-7}
E**	0.223	0.186
G***	1.50×10^{-5}	1.51×10^{-5}
Average***		
k_{ox}	12.8 ± 4.7 yr^{-1}	—
k_{red}	$(1.99 \pm 0.31) \times 10^{-3}$ yr^{-1}	—

* Strict best fit parameters could not be calculated because of limited pore water data. However, as shown in figures 5 and 6 and discussed in the text, these rate constants give reasonable profiles.

** See eqs (24) to (26) and the data in table 2.

*** See the text for an explanation of how these values were calculated.

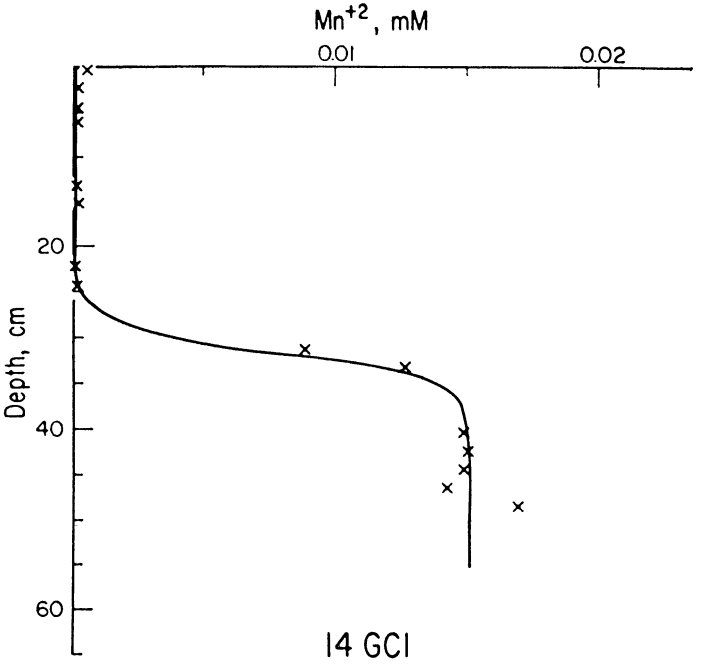

Fig. 3. Plot of pore water Mn^{2+} versus depth for core 14 GCI and the "best fit" curve predicted by eqs (17) and (18) using the parameters listed in table 2, $k_{ox} = 12.0$ yr^{-1} and $k_{red} = 2.10 \times 10^{-3}$ yr^{-1}.

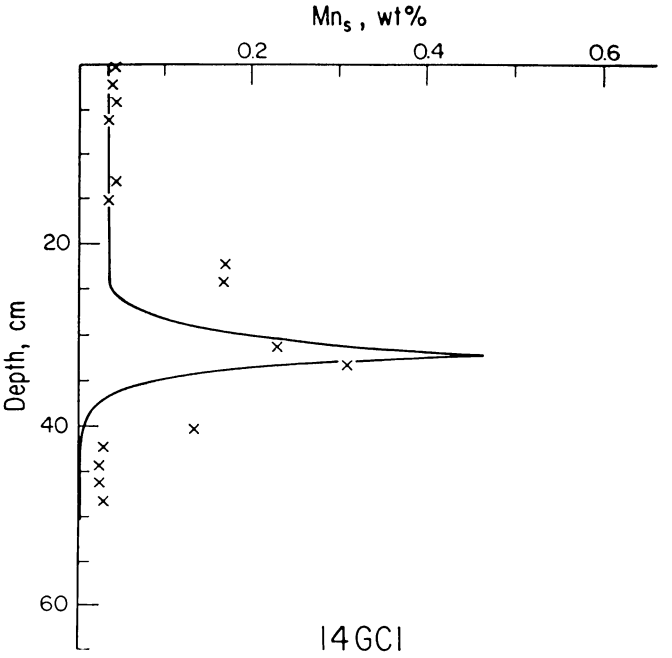

Fig. 4. Plot of solid phase Mn versus depth for core 14 GCI and the best fit curve predicted by eqs (19) and (20) using the parameters listed in table 2, $k_{ox} = 12.0$ yr^{-1} and $k_{red} = 2.10 \times 10^{-3}$ yr^{-1}.

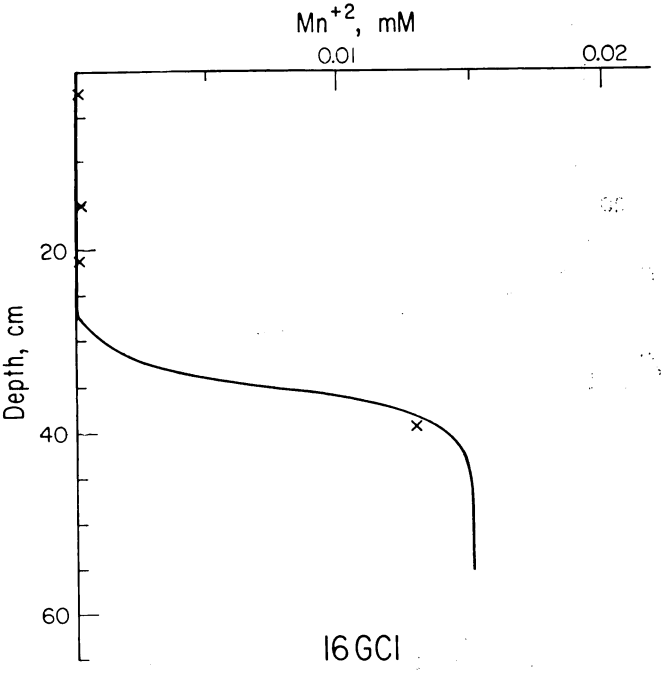

Fig. 5. Plot of pore water Mn^{+2} versus depth for core 16 GCI and the curve predicted by eqs (19) and (20) using the parameters listed in table 2, $k_{ox} = 10.7\ yr^{-1}$ and $k_{red} = 1.50 \times 10^{-3}\ yr^{-1}$.

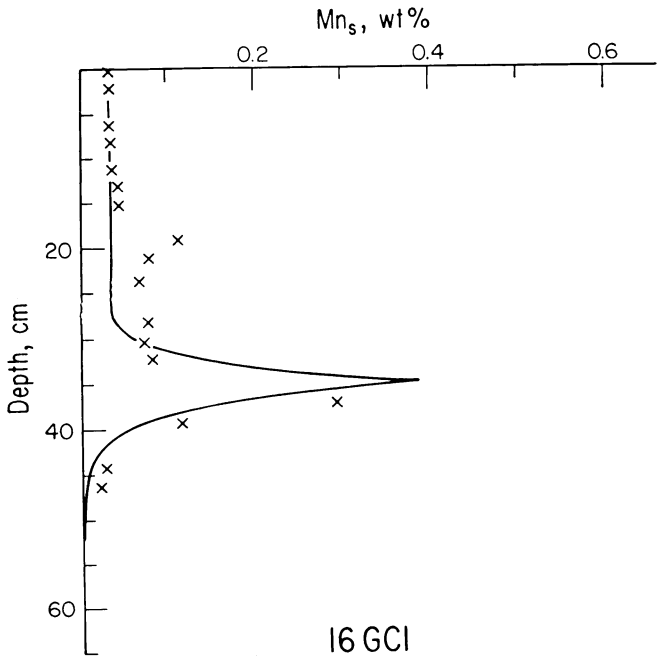

Fig. 6. Plot of solid phase Mn versus depth for core 16 GCI and the curve predicted by eqs (17) and (18) using the parameters listed in table 2, $k_{ox} = 10.7\ yr^{-1}$ and $k_{red} = 1.50 \times 10^{-3}\ yr^{-1}$.

certainties (1σ) of these two sets of rate constants are also shown in table 3. Profiles calculated with these "average" rate constants do not differ significantly from those shown in figures 3 and 4.

With 16 GC1, the lack of detailed pore water Mn data makes it impossible to go through the same type of calculations with the rate constants as we did in 14 GC1. However, using the parameters listed in table 2 and rate constants similar to those found in 14 GC1 (listed in table 3) curves are generated (figs. 5 and 6) which appear reasonable and in the case of solid manganese (where more detailed data are available) give a reasonably good fit.

DISCUSSION

As can be seen in figures 3 to 6, the fit to the pore water data is generally better than the fit of the solid data. Above the redox boundary, this may be due to episodic or short-term events that affect only the solids. These types of situations are discussed in greater detail in the next section.

Below the redox boundary, we see that the solid Mn data are consistently higher than the model profiles predict. Possible explanations include:

1. That there is more than one oxidation product formed in these sediments, and these products are reduced at different rates. Klinkhammer and Bender (1980), in discussing the distribution of manganese in the Pacific Ocean, suggest that the initial oxidation product in seawater is more similar to hausmanite (Mn_3O_4) than MnO_x ($x \approx 2$), which is consistent with the laboratory studies of Morgan (1967). Hem (1981) has also noted that under some conditions both hausmanite and feitnechite (β-MnOOH) can form in laboratory oxidation experiments. Below the oxidizing zone, hausmanite may undergo the following disproportionation reaction:

$$Mn_3O_4 + 4H^+ \rightarrow MnO_2 + 2Mn^{+2} + 2H_2O \qquad (27)$$

which has also been shown to occur in the laboratory (Bricker, 1965). If this also occurs in these sediments and the MnO_2 is then subsequently reduced to Mn^{+2}, the rate expression in the reducing zone will be far more complicated than eq (6) and may significantly modify the solid Mn profile.

2. Even if there is only one type of oxide present, eq (6) may be inappropriate for expressing the *in situ* rate law, particularly if reduction is microbially mediated. Other quantities which change with depth in the sediments (such as organic carbon or pH) may significantly affect the rate of reduction and therefore may need to be explicitly included in the rate expression. This would again imply that eq (6) is not appropriate and could explain the discrepancy between the predicted and measured solid profiles.

3. Manganese adsorption (which we have neglected) is important in the reducing zone.

4. There are residual amounts of Mn(II) in other mineral phases (such as silicate or carbonates, Stumm and Morgan, 1981) which are not involved in these redox reactions.

5. Non-steady state events (see next section) that have become buried below the redox boundary (as in 5 GC1, 10 GC1, and 23 GC1 (?)). We believe that this last suggestion is not likely because of the excellent fit of the pore water data in 14 GC1, the very reasonable fit to the solids data, and the resulting rate constants, which agree well with other calculated rates. This belief is further strengthened by our inability to obtain reasonable fits (using realistic parameters and rate constants) for either the pore-water or solids data of 5 GC1, 10 GC1, or 23 GC1, where evidence for a non-steady state is much stronger.

With regard to suggestions (1), (3), and (4), more detailed studies of manganese in the solids and a better understanding of manganese mineralogy are necessary. In addition, manganese reduction as both a biological and inorganic process must be better understood before the second suggestion (as well as part of the first) can be more critically examined. These types of studies (which are discussed below) are necessary to determine the relative importance of these suppositions for their eventual incorporation into future models.

The importance of short-term events on solid phase profiles and the steady state of the system

Short term events in this system, such as slumps, turbidity currents, or temporary fluctuations in the input of solid manganese to the sediments, will probably only affect the solid phase profiles, because diffusion is usually sufficiently rapid in re-establishing steady state gradients in the pore waters (Lerman, 1971). These effects (when they do disrupt the solid manganese depth profile) will also not affect the apparent steady state of the pore waters until after such an event is buried below the redox boundary and becomes involved in the remobilization we spoke of earlier. In 14 GC1 and 16 GC1 this may be the case (see figs. 4 and 6) where there appears to be a second maximum in solid manganese above the redox boundary, at around 20 and 24 cm, respectively. Until these peaks are buried below the redox boundary (and begin to dissolve via reduction) the pore water profiles can still be treated as if they are in steady state even though the overall manganese system is not (because this peak is moving downward with time).

In situations such as this, we feel it is still valid to use a steady state approach in modeling the system and obtaining reaction rates, since these fluctuations in the solids are still, in a sense, only "added on" to the steady state profile. However, it is for these reasons that we consider only the variance of the pore water data with calculated profiles in obtaining the best fit steady state rate constants. We use the word "only" with some degree of caution since one should certainly be concerned if this method resulted in solid phase profiles that showed extremely poor correlation with the actual data. In 14 GC1 and 16 GC1, this appears not to be the case.

When these types of fluctuations in the solids are ultimately buried below the redox boundary, the steady state of the pore waters and solids (both individually and together) is destroyed, and our model is no longer

applicable, because both profiles will now be time dependent. As we have discussed before, this appears to be the case in 5 GC1, 10 GC1, and 23 GC1. Attempts at fitting the data from Li, Bischoff, and Mathieu (1969) also imply similar conclusions.

Comparison of calculated rate constants with literature values

The oxidation rate constants calculated with this model are of the same order or slightly less than experimentally determined constants measured in the presence of solids such as calcite, feldspathic sand, or hydrous iron oxides (Hem, 1963, 1964, 1981; Michard, 1969). In all cases, these rates are much higher than those predicted by inorganic rate studies in the absence of abundant surface area (Hem, 1963; Morgan, 1967), most likely due to the catalytic effect of surfaces on oxidation. In summarizing these studies Boudreau and Scott (1978) suggest a lower limit for k_{ox} in marine sediments of $\approx 10^{-7}$ sec^{-1} ($= 3.2$ yr^{-1}), which agrees well with the constants calculated here (10.7 and 12.0 yr^{-1}).

As we have mentioned earlier, these reactions may also be catalyzed by microorganisms, although analogous rate constants and/or expressions for manganese oxidation by viable bacteria are not available for comparison. However, rate constants for manganese oxidation in seawater at 25°C by dormant spores of a marine *Bacillus* can be calculated from the data of Rosson and Nealson (1982). By applying an integrated form of eq (5) to the data in figure 2A of their paper, we have obtained a k_{ox} of about 75 yr^{-1}, which agrees well with our calculated rate constants. It should be pointed out that this correlation may perhaps be fortuitous as Rosson and Nealson (1982) also show that the kinetics of manganese oxidation by spores (and hence the apparent rate constant) is critically dependent on the number of spores present.

In laboratory studies with Long Island sound sediments, Aller (ms) obtained a k_{ox} of ≈ 50 yr^{-1}, while Elderfield and others (1981) calculated a rate constant of around 1000 yr^{-1} from laboratory flux studies with Narragansett Bay sediments. In addition, Emerson, Cranston, and Liss (1979), in studying water column manganese profiles in Saanich Inlet, estimate that k_{ox} is 180 yr^{-1}. In this environment manganese oxidation is presumed to be first-order due to a manganese rich particulate layer at the oxic-anoxic interface in the water column. These constants are all larger than those we have calculated for eastern equatorial Atlantic sediments and may be related to differences in the mechanism of manganese oxidation in these systems (that is, bacterial versus inorganic catalysis). In addition, these differences could be related to temperature differences between these four environments.

Similar comparisons of reduction rate constants are not possible as analogous laboratory studies have not, to our knowledge, been reported. However, the values calculated here can be compared with other model calculations. Holdren, Bricker, and Matisoff (1975), modelling pore water data and using a rate expression identical with ours (eq 6), obtained $k_{red} = 0.0173$ yr^{-1} for Chesapeake Bay sediments, while Aller (1980) in examining solid phase manganese profiles in Long Island Sound sediments

calculated that k_{red} was between 8.2 and 25 yr^{-1}. As can be seen from table 3, these results are higher than the k_{red} values we have calculated for sediments of the eastern equatorial Atlantic.

If reduction is indeed related to bacterial metabolism, then the lower rate in pelagic sediments could reflect the lower reactivity of organic matter in this environment (Berner, 1980). On the other hand, if reduction is abiogenic, these differences may be related to differences in the surface area and/or mineralogy of the solids involved in reduction in the two environments. In addition, in either case differences in rates could be related to temperature differences between near-shore and pelagic sediments.

Use of this model in determining the mechanisms of manganese redox reactions

In light of the previous section, it should be apparent that by itself this model is unable to discern bacterial from inorganic manganese reactions in marine sediments. One approach in distinguishing the two is to measure independently bacterial catalysis of these reactions (discussed in Nealson, 1983) along with pore water and solid profiles (to obtain the overall reaction rates). Assuming the bacterial reactions are also pseudo-first order, one should then be able to deduce the relative importance of bacterial catalysis, because given these assumptions,

$$k^{model} = k^{bact} + k^{inorganic} \tag{28}$$

for either oxidation or reduction.

It would also appear that continued laboratory studies of the "pure endmember" bacterial and inorganic reactions would be appropriate with specific regard to general rates and rate laws under *in situ* conditions (for both reactions), surface effects (for oxidation), and the effects of different manganese mineral phases on the rate of reduction. These would be very important in providing baseline data against which *in situ* results can be compared and in providing a better understanding of mechanisms and rate expressions for these reactions.

CONCLUSION

A steady state diagenetic model has been presented that accounts for changes in pore water and solid phase manganese profiles in marine sediments due to advection, diffusion and redox reactions. When applied to actual manganese distributions in sediments (both in pore waters and solids) one is able to obtain *in situ* reaction rates for manganese oxidation and reduction.

The model has been applied to two sedimentary cores in the eastern equatorial Atlantic, and very good fits to the data have been obtained. The resulting rate constants appear to be consistent with other calculated constants. It is hoped that in the future this model can be applied to additional cores to test the range of its applicability and validity.

By itself, the model provides limited insight into the exact mechanisms of these redox processes in marine sediments. However, when

combined with appropriate laboratory and field studies the relative importance of inorganic versus bacterially mediated manganese transformation in these systems should become more clear.

ACKNOWLEDGMENTS

We thank Drs. R. E. McDuff and P. Kepkay for reading the manuscript. Mr. B. Boudreau critically reviewed an earlier version. This research was supported by NSF Grant OCE 78-27376 (MANOP).

APPENDIX

Derivation of equations (17) to (26)

If eq (7) is solved and boundary condition (1) is applied to the solution we obtain:

$$C_p^{ox} = B(e^{\alpha(z-L1)} - e^{-\alpha(z-L1)}) = A\sinh(\alpha(z-L1)) \qquad \text{(A1) and (17)}$$

where A and B are constants (A = B/2) and

$$\alpha = \frac{w \pm \sqrt{w^2 + 4k_{ox}D_b}}{2D_b} \approx \sqrt{\frac{k_{ox}}{D_b}} \qquad \text{(A2) and (21)}$$

assuming $4D_bk_{ox} >> w^2$. If eq (A1) is used in solving eq (8) and boundary condition (2) (eq 12) is applied to this solution, we obtain

$$C_s^{ox} = \frac{k_{ox}\phi A}{\alpha w(1-\phi)}(\cosh(\alpha(z-L1)) - 1) + C_s^{\circ} \qquad \text{(A3)}$$

Solving eq (10) we obtain

$$c_s^{red} = Ee^{-\beta(z-L2)} \qquad \text{(A4) and (20)}$$

If this equation is substituted into eq (9) we obtain

$$C_p^{red} = G + He^{w(z-L2)/D_b} - \frac{1-\phi}{\phi}\frac{k_{red}E}{D_b\beta^2 + w\beta}e^{-\beta(z-L2)} \qquad \text{(A5)}$$

where $\beta = k_{red}/w$ (eq 22). Application of boundary condition (5) implies H = 0 and if we also assume that $D_bk_{red} >> w^2$, we obtain

$$C_p^{red} = G - \frac{1-\phi}{\phi}\frac{Ew^2}{k_{red}D_b}e^{-\beta(z-L2)} \qquad \text{(A6) and (18)}$$

Now if boundary conditions (2) and (3) (eqs 13, 14, and 16) are applied to eqs (A1), (A3), (A4), and (A6) we obtain the following:

$$\text{Asinh}\,\alpha L_{ox} = G - \frac{1-\phi}{\phi}\frac{Ew^2}{k_{red}D_b} \qquad \text{(A7)}$$

(pore water conc. continuity)

$$\frac{k_{ox}\phi A}{\alpha w(1-\phi)}(\cosh\alpha L_{ox} - 1) + C_s^{\circ} = E \qquad \text{(A8)}$$

(solid conc./flux continuity)

$$A\cosh\alpha L_{ox} = \frac{1-\phi}{\phi}\frac{Ew}{D_b} \qquad \text{(A9)}$$

(pore water flux continuity)

Where L_{ox} = L2-L1 (eq 23). Eqs (A8) and (A9) can be used to solve for A and E giving

$$A = \frac{1-\phi}{\phi}\frac{C_s^{\circ}w}{\alpha D_b} \qquad \text{(A10) and (24)}$$

$$E = C_s^{\circ}\cosh\alpha L_{ox} \qquad \text{(A11) and (25)}$$

If this expression for A is substituted into eq (A3), the equation simplifies to

$$C_s^{ox} = C_s^{\circ}\cosh(\alpha(z-L1)) \qquad \text{(A12) and (19)}$$

If eq (A10) is then substituted into eq (A7), the expression becomes

$$G = A(\sinh\alpha L_{ox} + \alpha/\beta\cosh\alpha L_{ox}) \qquad \text{(A13) and (26)}$$

and we have now obtained the solutions described by eqs (17) to (26).

REFERENCES

Aller, R. C., ms, 1977, The influence of macrobenthos on chemical diagenesis of marine sediments: Ph.D. thesis, Yale Univ., 600 p.

———— 1980, Diagenetic processes near the sediment water interface of Long Island Sound sediments. II. Fe and Mn: Adv. Geophysics, v. 22, p. 351-415.

Bender, M. L., 1971, Does upward diffusion supply the excess manganese in pelagic sediments?: Jour. Geophys. Research, v. 76, p. 4212-4215.

Berner, R. A., 1980, Early Diagenesis, A Theoretical Approach: Princeton, N.J., Princeton Univ. Press, 241 p.

Bischoff, J. L., and Sayles, F. L., 1972, Pore fluid and mineralogical studies of recent marine sediments: Bauer depression region of East Pacific Rise: Jour. Sed. Petrology, v. 42, p. 711-724.

Bricker, O. P., 1965, Some stability relationships in the system $Mn–O_2–H_2O$ at 25°C and 1 atm total pressure: Am. Mineralogist, v. 50, p. 1296-1354.

Boudreau, B. P., and Scott, M. R., 1978, A model for the diffusion-controlled growth of deep sea manganese nodules: Am. Jour. Sci., v. 278, p. 903-929.

Claypool, G. E., and Kaplan, I. R., 1974, The origin and distribution of methane in marine sediments, *in* Kaplan, I. R., ed., Natural Gases in Marine Sediments: New York, Plenum Press, p. 99-139.

Elderfield, H., Luedtke, N., McCaffrey, R. J., and Bender, M., 1981, Benthic flux studies in Narragansett Bay: Am. Jour. Sci., v. 281, p. 768-787.

Emerson, S., Cranston, R. E., and Liss, P. S., 1979, Redox species in a reducing fjord: equilibrium and kinetic considerations: Deep-Sea Research, v. 26A, p. 859-878.

Emerson, S. A., Jahnke, R., Bender, M., Froelich, P., Klinkhammer, G., Bowser, C., and Setlock, G., 1980, Early diagenesis in sediments from the Eastern Equatorial Pacific. I. Pore water nutrients and carbonate results: Earth Planetary Sci. Letters, v. 49, p. 57-80.

Emerson, S. A., Jacobs, L., Kalhorn, S., Nealson, K. H., Rosson, R. A., and Tebo, B. M., 1982, Environmental oxidation rate of manganese (II): Bacterial catalysis: Geochim. et Cosmochim. Acta, v. 46, p. 1073-1079.

Froelich, P. N., ms, 1980, Marine phosphorus geochemistry: Ph.D. thesis, Univ. Rhode Island, 291 p.

Froelich, P. N., Klinkhammer, G. P., Bender, M. L., Luedtke, N. A., Heath, G. R., Cullen, D., Dauphin, P., Hammond, D., Hartman, B., and Maynard, V., 1979, Early oxidation of organic matter in pelagic sediments of the eastern equatorial Atlantic: suboxic diagenesis: Geochim. et Cosmochim. Acta, v. 43, p. 1075-1090.

Hem, J. D., 1963, Chemical equilibrium and rates of manganese oxidation: U.S. Geol. Survey Water Supply Paper 1667A, p. 1-61.

———— 1964, Deposition and solution of manganese oxides: U.S. Geol. Survey Water Supply Paper 1667B, p. 1-42.

———— 1981, Rates of manganese oxidation in aqueous systems: Geochim. et Cosmochim. Acta, v. 45, p. 1369-1374.

Holdren, G. R., Jr., Bricker, O. P. III, and Matisoff, G., 1975, A model for the control of dissolved manganese in the interstitial waters of Chesapeake Bay, *in* Church, T. M., ed., Marine Chemistry in the Coastal Environment: Washington, D.C., Am. Chem. Soc. Symposium ser. 18, p. 364-381.

Klinkhammer, G. P., 1980, Early diagenesis in sediments from the eastern equatorial Pacific, II. Pore water metal results: Earth Planetary Sci. Letters, v. 49, p. 81-101.

Klinkhammer, G. P., and Bender, M. L., 1980, The distribution of manganese in the Pacific Ocean: Earth Planetary Sci. Letters, v. 46, p. 361-384.

Lerman, A., 1971, Time to chemical steady states in lakes and oceans, *in* Hem, J. D., ed., Nonequilibrium Systems in Natural Water Chemistry: Washington, D.C., Adv. Chemistry Series 106, p. 30-77.

Li, Y.-H., Bischoff, J., and Mathieu, G., 1969, The migration of manganese in the Arctic basin sediments: Earth Planetary Sci. Letters, v. 7, p. 265-270.

Li, Y.-H., and Gregory, S., 1974, Diffusion of ions in seawater and in deep-sea sediments: Geochim. et Cosmochim. Acta, v. 38, p. 703-714.

Lynn, D. C., and Bonatti, E., 1964, Mobility of manganese in diagenesis of deep-sea sediments: Marine Geology, v 3, p. 457-474.

McDuff, R. E., and Ellis, R. A., 1979, Determining diffusion coefficients in marine sediments: a laboratory study of the validity of resistivity techniques: Am. Jour. Sci., v. 279, p. 666-675.

McDuff, R. E., and Gieskes, J. M., 1976, Calcium and magnesium profiles in DSDP interstitial waters: diffusion or reaction?: Earth Planetary Sci. Letters, v. 33, p. 1-10.

Michard, G., 1969, Depot de traces de manganese par oxidation: Acad. Sci. Paris Comptes Rendus, v. 269, ser. D., p. 1811-1814.

———— 1971, Theoretical model for manganese distribution in calcareous sediment cores: Jour. Geophys. Research, v. 76, p. 2179-2186.

Morgan, J. J., 1967, Chemical equilibrium and kinetic properties of manganese in natural waters, *in* Faust, S. C., and Hunter, J. V., eds., Principals and Applications of Water Chemistry: New York, John Wiley & Sons, p. 561-624.

Nealson, K. H., 1983, The microbial manganese cycle, *in* Krumbein, W. E., ed., Biogeochemistry, in press.

Peng, T. H., Takahashi, T., and Broecker, W. S., 1974, Surface radon measurements in the north Pacific Ocean station Papa: Jour. Geophys. Research, v. 79, p. 1772-1780.

Robbins, J. A., and Callender, E., 1975, Diagenesis of manganese in Lake Michigan sediments: Am. Jour. Sci., v. 275, p. 512-533.

Rosson, R. A. and Nealson, K. H., 1982, Manganese binding and oxidation by spores of a marine *Bacillus*: Jour. Bacteriology, v. 151, p. 1027-1034.

Stumm, W., and Morgan, J. J., 1981, Aquatic Chemistry: New York, Wiley-Intersci., 780 p.

Wadsworth, W. D., 1975, Reactions at surfaces, *in* Eyring, H., ed., Physical Chemistry, v. 7: New York, Academic Press, p. 417-473.

Wollast, R., Billen, G., and Duinker, J. C., 1979, Behavior of manganese in the Rhine and Scheldt Estuaries: Estuarine Coastal Marine Sci., v. 9, p. 161-169.